Arab J Geosci (2016) 9: 298
DOI 10.1007/s12517-016-2316-y

ORIGINAL PAPER

Application of fuzzy analytical hierarchy process (AHP) and prediction-area (P-A) plot for mineral prospectivity mapping: a case study from the Dananhu metallogenic belt, Xinjiang, NW China

Xishihui Du[1,2] · **Kefa Zhou**[1] · **Yao Cui**[1,3] · **Jinlin Wang**[1] · **Nannan Zhang**[1] · **Weidong Sun**[4]

Received: 31 October 2015 / Accepted: 11 January 2016 / Published online: 31 March 2016

Abstract This paper describes a GIS-based application of a fuzzy analytical hierarchy process (AHP) to map porphyry-Cu prospectivity in the Dananhu metallogenic belt, NW China. Based on a model of porphyry-Cu mineralization, evidential layers were derived from geological, geochemical, and geophysical data. These layers were subsequently assigned weights by implementing a fuzzy AHP method using knowledge from three experts in porphyry-Cu exploration. After obtaining normalized weights, different fuzzy operators were tried to combine the weighted evidential layers into potential maps, which were then compared and evaluated by predication-area (P-A) plots. Subsequently, a ternary map was generated by defuzzification of the optimum prospectivity map as selected by the P-A plot; this ternary map shows zones of high, moderate, and low favorability for porphyry-Cu deposits in the study area. To further evaluate the results, potential zones were analyzed for two-dimensional spatial domain. The results demonstrate that the fuzzy AHP method can be effectively applied to mineral prospectivity mapping in vaguely known areas.

✉ Kefa Zhou
zhoukf@ms.xjb.ac.cn

[1] Xinjiang Research Center for Mineral Resources, Xinjiang Institute of Ecology and Geography, Chinese Academy of Sciences, Urumqi 830011, China

[2] University of Chinese Academy of Sciences, Beijing 100049, China

[3] British Columbia Geological Survey, Victoria, BC V8W 9N3, Canada

[4] Information Center of Bureau of Geology and Mineral Resources of Xinjiang, Urumqi 830046, China

Keywords Fuzzy analytical hierarchy process · Mineral prospectivity mapping · Porphyry-Cu deposits · Dananhu metallogenic belt

Introduction

Mineral prospectivity mapping (MPM) aims to delineate target areas that are most likely to contain mineral deposits of a certain type in the region of interest. To achieve this goal, one of the challenges in MPM is to assign weights to the individual evidential layers that are used as indictors. A variety of methods are used to weight individual evidential layers and to integrate them into a single potential map. These methods can be categorized into three types (Bonham-Carter 1994; Carranza 2008; Yousefi and Carranza 2015c). (1) Knowledge-driven MPM methods qualitatively assess the relationship between each evidential layer and the presence of deposits of the type sought based on expert knowledge. Boolean logic (Bonham-Carter 1994), index overlay (Carranza et al. 1999), fuzzy logic (An et al. 1991; Knox-Robinson 2000), wildcat mapping (Carranza and Hale 2002; Carranza 2010), and outranking method (Abedi et al. 2013a) are examples of knowledge-driven MPM methods, which are properly used in frontier or less-explored areas (so-called greenfields) with no or very few mineral deposits of the desired type. (2) Data-driven MPM methods analyze and quantify spatial associations between each evidential layer and the locations of known deposits that share a common genesis. The ultimate aim of this process is to obtain a mineral potential map by combining quantified spatial associations. Data-driven MPM methods include weights of evidence (Liu et al. 2014; Zuo 2011), evidence belief functions (Carranza 2014; Carranza and Hale 2003; Liu et al. 2015), logistic

regression (Agterberg and Bonham-Carter 1999; Carranza and Hale 2001), neural networks (Porwal et al. 2003a; Singer and Kouda 1996), etc. These methods are commonly applied in well-explored areas with sufficient known mineral deposits of the type sought. (3) There are other methods that assign weights to evidential layers using neither known mineral occurrences nor the judgments of experts (Yousefi and Carranza 2014, 2015a, b, c; Yousefi and Nykänen 2015).

The knowledge and data-driven MPM methods each have their weaknesses in application. In terms of data-driven methods, enough known mineral deposits are needed as "training points" to ensure well performance. For the knowledge-driven methods, the assignment of meaningful weights to each evidential layer is a highly subjective exercise that usually involves trial and error, even in cases where "real-expert" knowledge is available, and particularly when a number of different experts are involved. Nevertheless, the analytical hierarchy process (AHP) proposed by Saaty (1980) can resolve this difficulty in evaluating the relative importance of each evidential layer, aided by making pairwise comparisons (Carranza 2008). In addition, this method is straightforward for decision-makers (DMs) to use to structure a complex problem into a systematic hierarchy using the AHP technique. Despite of the above strengths, the AHP is criticized for expressing human judgment in crisp values in that DMs usually feel more confident to provide fuzzy judgments than crisp numbers (Dagdeviren 2008; Wang et al. 2008). As a result, fuzzy AHP and its extensions have been proposed to solve fuzzy justification problems (Laarhoven and Pedrycs 1983; Buckley 1985; Chang 1996; Xu 2000). Chang's (1996) extent analysis for fuzzy AHP is applied in this study, which has proved to be a useful tool in mineral prospectivity mapping (Abedi et al. 2013b; Najafi et al. 2014; Pazand et al. 2014).

The purpose of this study is to highlight high potential zones of porphyry-Cu deposits in the Dananhu metallogenic belt, NW China, where only five porphyry-Cu deposits have been discovered. For this purpose, a fuzzy AHP method was applied to determine the weights of 12 evidential layers obtained from geological, geochemical, and geophysical data, based on the opinions of three DMs who are professionals in porphyry-Cu exploration. Prospectivity maps were then generated by combining the weighted evidential layers using fuzzy operators. Subsequently, prediction-area (P-A) plot (Yousefi and Carranza 2014, 2015a, b, c; Yousefi and Nykänen 2015) was then used for comparison and evaluation of the results to obtain the optimum result, and concentration-area (C-A) model (Cheng et al. 1994) was used to determine the thresholds of the optimum result for getting a ternary prospectivity map (Yousefi and Carranza 2015b, c; Yousefi and Nykänen 2015). Ultimately, the ability of the applied method was demonstrated in a spatial domain.

Study area

Geological setting

The study area is located in the southern margin of the Turfan-Hami (commonly abbreviated as TuHa) Basin in eastern Tianshan, which contains parts of the Dananhu metallogenic belt (Dong et al. 2010) and covers an area of about 15,800 km^2 (Fig. 1). The region is characterized by extensive occurrences of Quaternary gravel and aeolian sand covering an area of more than 6500 km^2, in which a number of massive sulfide and porphyry copper-zinc deposits were discovered. The region is chiefly composed of Devonian to Carboniferous volcanic and intrusive rocks with several genetically affiliated porphyry-Cu deposits of different sizes, including the Yandong, Tuwu, Linglong, and Chihu deposits (Zhang et al. 2006). The base of the belt is represented by basaltic to andesitic volcanic rocks, with locally overlying Lower Carboniferous carbonates and calcareous mudstones (Mao et al. 2005). The structures of the region are dominated by a series of NW- and NE-trending strike-slip faults, including the Kanggurtag fault and the Dacaotan fault. Permian and older strata have been regionally metamorphosed to lower greenschist and prehnite-pumpellyite facies (Han et al. 2006). As far as the geological setting, the Dananhu metallogenic belt is similar to the Gobi desert of southern Mongolia, in which a world-class Oyu Tolgoi Cu–Au–Mo porphyry deposit was discovered. Generally, the Dananhu metallogenic belt has prospective potential for porphyry-Cu deposits (Zhang et al. 2006).

Porphyry-Cu mineralization model

Porphyry-Cu deposits are formed by magmatic-hydrothermal transport of metals along fractured conduits within porphyritic intrusive rocks. Commonly, once the magma solidifies, hydrothermal fluids are converted into porphyries and its surrounding host rocks (Lindsay et al. 2014; Yousefi and Carranza 2014).

In the Dananhu metallogenic belt, the heat sources for porphyry-Cu mineralization were Carboniferous to Permian intermediate-acid porphyritic intrusions, such as plagiogranite and dioritic porphyrite, which provided heat and metal-bearing magmatic-hydrothermal fluids for porphyry-Cu mineralization (Zhu 2003). The emplacement of deposits is predominantly controlled by proximity to NE-trending regional faults, which facilitate the channeling of magma and the circulation of hydrothermal fluids. In particular, the most important structural zone, the Kanggurtag and Dacaotan faults along which intense deformation, magmatic activity, and associated mineralization took place, can be regarded as a favorable indicator for the occurrence of porphyry-Cu deposits. Chen (2006) and Xiao (2013) indicate that the porphyry-Cu mineralization is mainly hosted within Carboniferous intermediate–basic volcanic rocks. In the formation of porphyry-Cu

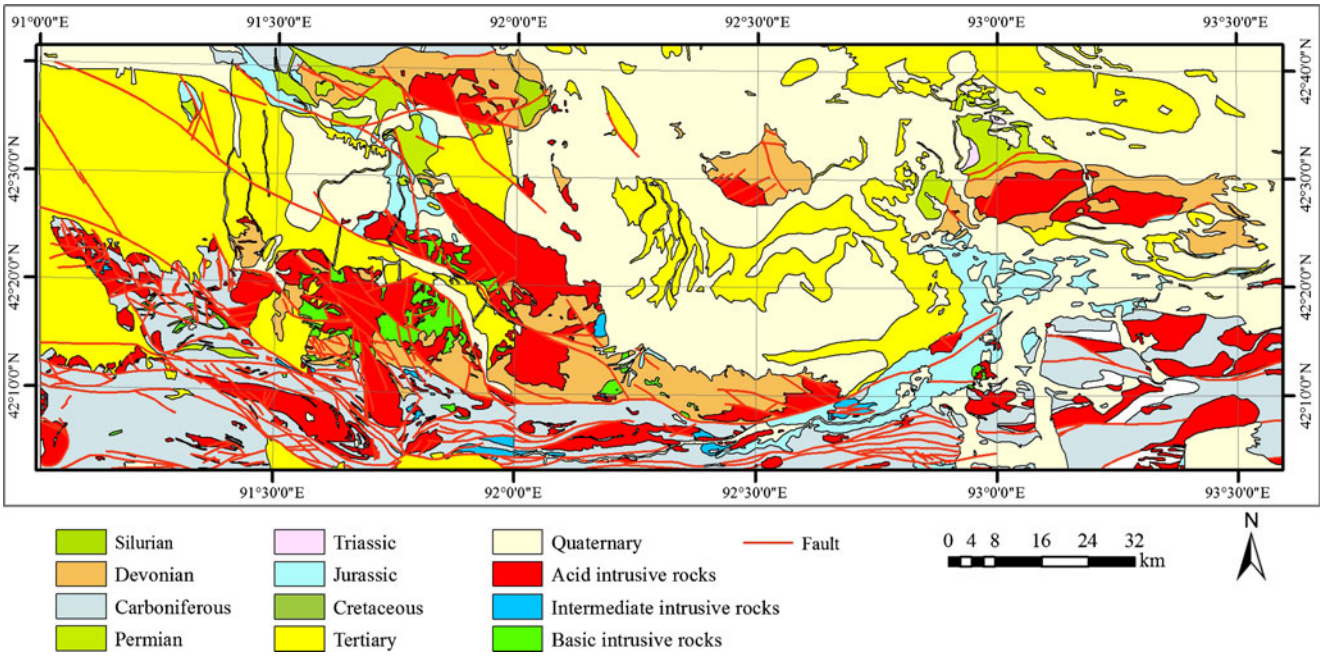

Fig. 1 Simplified geological map of the study area (modified from Bureau of Geology and Mineral Resources of Xinjiang)

deposits, the process is commonly accompanied by hydrothermal alteration. The pattern of this alteration is characterized by sericite, silicified, pyritized, and propylitic alteration. Mineralogy and geochemistry show that the ore-bearing plagiogranite porphyries have an affinity with the early Carboniferous adakitic tonalitic rocks. It indicates that early Carboniferous tonalitic rocks play an important role for porphyry-Cu mineralization (Wang et al. 2015; Zhang et al. 2006). To summarize, the occurrence of heat sources, regional faults, favorable host rocks, and alteration are essential for the deposition of porphyry-Cu mineralization. The mineral assemblages of porphyry-Cu mineralization exhibit high concentrations of Ag, Au, Cu, Mo, Pb, and Zn, which are indicator elements for porphyry-Cu mineralization (Xiao 2013; Zhuang 2003; Zhuang et al. 2003). Additionally, geophysical anomalies in the airborne magnetic and Bouguer gravity data, represented by locally high magnetic and low gravity data, are symptomatic of porphyry-Cu mineralization (Zhu et al. 2003; Zhuang et al. 2003). The characteristics of porphyry-Cu mineralization discussed above are considered as a model that informs the choice of spatial data as evidential layers.

A typical Porphyry-Cu deposit

The Tuwu porphyry-Cu deposit, which reserves about 2.04 million tons of copper at an average grade of 0.67 % Cu, is one of the largest porphyry-Cu deposits in western China (Liu et al. 2003; Wang et al. 2001). The Tuwu deposit is hosted in the Carboniferous Qi'eshan Group, which can be divided into three sections. The lowest section, exposed north of the Kanggurtag fault, is composed of volcaniclastics and tuff with minor biolithite and glutenite. The middle section is represented by basalt, andesite, and dacite. The composition of volcanic rocks varies from calc-alkaline to alkaline. The upper section, distributed south of the Dacaotan fault, is mainly composed of sandstone and basalt with intercalated tuff and andesite (Wang et al. 2001). The ore-bearing plagiogranite porphyries yielded SHRIMP zircon U–Pb ages of 333 ± 2 Ma and Re–Os isochron ages of 323 ± 2.3 Ma (Liu et al. 2003; Rui et al. 2002a). Primary fluid inclusion indicates that mineralizing temperatures are of 150 to 280 °C (Rui et al. 2002b). The mineral assemblages are chiefly chalcopyrite, pyrite, chalcocite, molybdenite, quartz, and sericite. Wall-rock alteration is divided into five zones from the core to the margin in sequence: quartz core zone, biotite zone, phyllic zone, argillite zone, and propylitic zone (Wang et al. 2001).

Data and method

Data

In this study, the spatial dataset was derived from established multi-source geological spatial databases containing geological, geochemical, and geophysical data. Geological maps at a scale of 1:200,000 were collected from the Bureau of Geology and Mineral Resources of Xinjiang. The stream sediment geochemical data at a 1:200,000 scale were obtained from the National Geochemical Mapping Project of China (Xie et al. 1997). Geophysical datasets include Bouguer gravity data and airborne magnetic intensity data with a 2-km spatial resolution.

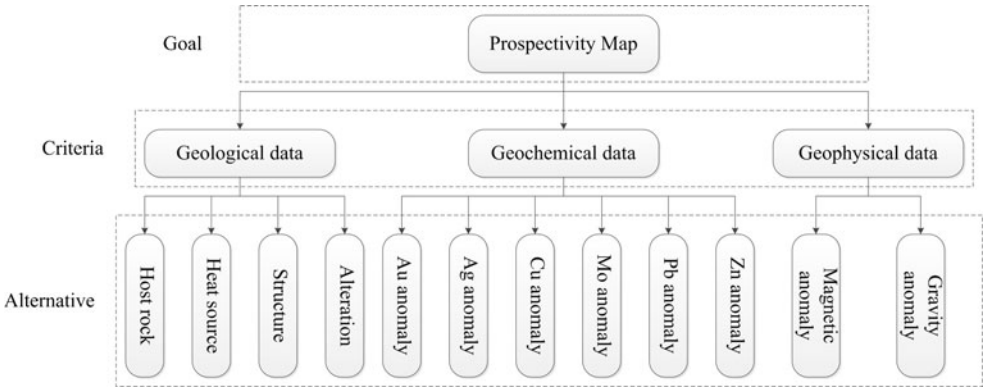

Fig. 2 Hierarchical structure of mineral prospectivity mapping

Fuzzy AHP method

This study presents the extent fuzzy AHP (Chang 1996), in which the weights of the nine-level fundamental scales of judgments are expressed via the triangular fuzzy numbers (TFNs) in order to represent the relative importance among the hierarchy criteria (Karimi et al. 2011).

The steps involved in applying the fuzzy AHP in MPM based on the paper published by Abedi et al. (2013b) are summarized as follows.

Step 1. Construction of a hierarchy

In the first step, a complex decision problem is simplified into a hierarchy of interrelated decision elements (criteria, decision alternatives). A hierarchy has at least three levels: the first hierarchy is the goal; the middle hierarchy refers to multiple criteria that define alternatives; and the final hierarchy consists of decision alternatives (Albayrak and Erensal 2004). The hierarchical structure established to represent the interrelationships in MPM for this study is illustrated in Fig. 2.

Step 2. Construct pairwise comparison matrix

A group of t decision-makers (DM_p) compares pairwise criteria and alternatives according to their relative importance with respect to a proposition, and uses the fundamental comparison scale of nine levels (Table 1) (Carranza 2008). Each DM will individually construct a pairwise comparison matrix (PCM), as shown in Eq. (1), for each criterion:

$$DM_p = \begin{bmatrix} a_{11p} & a_{12p} & \cdots & a_{1mp} \\ a_{21p} & a_{22p} & \cdots & a_{2mp} \\ \vdots & \vdots & \vdots & \vdots \\ a_{m1p} & a_{m2p} & \cdots & a_{mmp} \end{bmatrix} p = 3, 4, \ldots, t, \quad (1)$$

where a_{ijp} is the quotient of weights of the alternatives, m is the number of alternatives for each criterion, and t is the number of DMs.

Step 3. Check for consistency ratio (CR)

If the pairwise comparison matrix $DM_p=(a_{ijp})_{m\times n}$ satisfies $a_{ijp}=a_{ikp}\times a_{kjp}$ for any $i, j, k=1,\ldots,m$, then DM_p is considered to be perfectly consistent; otherwise, it is said to be inconsistent. The consistency index (CI) is:

$$CI = \frac{\lambda_{max} - n}{n-1} \quad (2)$$

where λ_{max} is the maximum eigenvalue of DM_p.

The final consistency ratio (CR) determines whether the evaluations are sufficiently consistent, and is calculated as the ratio of the CI and the random index (RI) (Table 2):

Table 1 The fundamental scale for pairwise comparisons (Saaty 1980)

Intensity of importance	Definition
1	Equal importance
3	Moderate importance
5	Strong importance
7	Very strong importance
9	Extreme importance
2, 4, 6, 8	Intermediate values between the 2 adjacent judgments
Reciprocals of above values	If activity i has one of the above nonzero numbers assigned to it when compared with activity j, then j has the reciprocal value when compared with i.

Table 2 Random index (RI) (Saaty 1980)

	Number									
	1	2	3	4	5	6	7	8	9	10
RI	0.00	0.00	0.52	0.89	1.11	1.25	1.35	1.40	1.45	1.49

$$\mathrm{CR} = \frac{\mathrm{CI}}{\mathrm{RI}}$$

If CR≤0.1, the consistency of a pairwise comparison matrix is accepted; otherwise, the pairwise comparisons must be revised in step 2.

It should be noted that the consistency of the pairwise comparison judgments not only measures the consistency of decision makers but also evaluates the quality of the model (Albayrak and Erensal 2004; Pazand et al. 2014).

Step 4. Construct fuzzy evaluation matrix

A fuzzy number M on R is a TFN if its membership function $\mu_M(x):R\rightarrow[0, 1]$ is equal to

$$\mu_M(x) = \begin{cases} \dfrac{x}{m-l} - \dfrac{l}{m-l}, & x\in[l,\ m], \\ \dfrac{x}{m-u} - \dfrac{u}{m-u}, & x\in[m,\ u], \\ 0, & \text{otherwise}, \end{cases} \tag{4}$$

where $l<<m<<u$, l and u stand for the lower and upper values of the support of M, respectively, and m gives the modal value of the membership function $\mu_M(x)$. The triangular fuzzy number can be denoted by $(l,\ m,\ u)$. The support of M is the set of elements $\{x\in R|l<x<u\}$ (Chang 1996).

First, a comprehensive PCM is constructed by integrating the grades of all DMs via Eq. (5). In this way, the PCM values of DMs are transformed into TFNs to make the fuzzy evaluation matrix:

$$l_{ij} = \min(a_{ijp}),\ \ m_{ij} = \sum_{p=1}^{t} \frac{a_{ijp}}{t},\ \ u_{ij} = \max(a_{ijp}),\ \ M_{ij} = (l_{ij},\ m_{ij},\ u_{ij})$$
$$p = 1, \ldots, t;\ i = 1, \ldots, m;\ j = 1, \ldots, m \tag{5}$$

where $\min(a_{ijp})$ and $\max(a_{ijp})$ indicate minimum and maximum values of the PCMs prepared by DMs for each i and j, respectively.

Second, compute the value of the fuzzy synthetic extent with respect to the ith object of m alternatives for each criterion via Eq. (6):

$$S_i = \sum_{j=1}^{m} M_{ij} \otimes \left[\sum_{k=1}^{m}\left(\sum_{j=1}^{m} M_{kj}\right)\right]^{-1} \quad i,\ j,\ k = 1, \ldots, m \tag{6}$$

where all the M_{ij} are TFNs after construction of the fuzzy evaluation matrix. Considering two TFNs, $M_1=(l_1,\ m_1,\ u_1)$ and $M_2=(l_2,\ m_2,\ u_2)$, their operational laws are as follows:

$$(l_1,\ m_1,\ u_1)\otimes(l_2, m_2, u_2)\approx(l_1 l_2, m_1 m_2, u_1 u_2) \tag{7}$$

$$(l_1, m_1, u_1)^{-1}\approx\left(\frac{1}{u_1}, \frac{1}{m_1}, \frac{1}{l_1}\right) \tag{8}$$

Third, calculate the degree of possibility (V) of $M_2>>M_1$ via Eq. (9):

$$V(M_2>>M_1) = \begin{cases} 1, & \text{if } m_2>>m_1 \\ 0, & \text{if } l_1>>u_2 \\ \dfrac{l_1-u_2}{(m_2-u_2)-(m_1-l_1)}, & \text{otherwise} \end{cases} \tag{9}$$

To compare M_1 and M_2, it is necessary to consider both values of $V(M_2>>M_1)$ and $V(M_1>>M_2)$.

Finally, the degree of possibility (V) that a convex fuzzy number is greater than k convex fuzzy numbers $M_i(i=1, 2,\ldots, k)$ can be defined by the following equation:

$$\begin{aligned} &V(M >> M_1, M_2, \ldots, M_k) \\ &\quad = V[(M >> M_1)\ and (M >> M_2)\ \text{and}\ldots\text{and}(M >> M_k)] \\ &\quad = \min V(M >> M_1) \quad i = 1,\ 2, \ldots, k \end{aligned} \tag{10}$$

Assume that $d(B_i)=\min V(S_i>>S_k)$, $k=1,\ldots,m$, and $k\neq i$. The weight vector is then given by

$$W' = (d'(B_1), \ldots, d'(B_m))^T \tag{11}$$

Where $B_i(i=1,\ldots,m)$ has m elements.

Step 5. Calculate normalized weights

Via normalization, the normalized weight vectors are

$$W = (d(B_1),\ \ldots,\ \mathrm{d}(B_m))^T \tag{12}$$

where W is a non-fuzzy number.

As pointed out by Wang et al. (2008), the weights determined by the extent analysis method do not represent the relative importance of decision criteria or alternatives and could not be used to give their priority, on condition that irrational zero weights are assigned to some useful decision criteria and alternatives.

Step 6. Using fuzzy operators

Table 3 Summary of classes and class scores with respect to evidence layers

Evidential layer	Class	Class score
Host rock	Volcanic rock (andesite, basalt, augite andesite)	10
	Buffer 1 km	8
	Buffer 2 km	6
	Buffer 3 km	4
Heat source	Intrusive rocks by a composition of diorite	10
	Buffer 1 km	8
	Buffer 2 km	6
	Buffer 3 km	4
	Intrusive rocks by a composition of monzodiorite	8
	Buffer 1 km	6
	Buffer 2 km	4
	Buffer 3 km	2
	Intrusive rocks by a composition of	A
	monzonite and quartz monzonite	o
	Buffer 1 km	4
	Buffer 2 km	2
	Buffer 3 km	1
Alteration	Silicified ± carbonated zone	10
	Buffer 0.5 km	8
	Buffer 1 km	6
	Buffer 1.5 km	4
	Hornfelsed ± silicified zone	7
	Buffer 0.5 km	5
	Buffer 1 km	3
	Buffer 1.5 km	2
	Zeolitic zone	4
	Buffer 0.5 km	3
	Buffer 1 km	2
	Buffer 1.5 km	1
Structure (fault)	Density >1.53 (length per unit area)	10
	Density 1.36–1.53 (length per unit area)	9
	Density 1.19–1.36 (length per unit area)	8
	Density 1.02–1.19 (length per unit area)	7
	Density 0.85–1.02 (length per unit area)	6
	Density 0.68–0.85 (length per unit area)	5
	Density 0.51–0.68 (length per unit area)	4
	Density 0.34–0.51 (length per unit area)	3
	Density 0.17–0.34 (length per unit area)	2
	Density 0–0.17 (length per unit area)	1
	Distance 0–1 km	7
	Distance 1–2 km	6
	Distance 2–3 km	5
	Distance 3–4 km	4
	Distance 4–5 km	3
	Distance 5–6 km	2
	Distance >6 km	1
Magnetic intensity	Magnetic intensity l	10
	Magnetic intensity 2	9
	Magnetic intensity 3	8
	Magnetic intensity 4	7
	Magnetic intensity 5	6
	Magnetic intensity 6	5
	Magnetic intensity7	4
	Magnetic intensity 8	3
	Magnetic intensity 9	2
	Magnetic intensity 10	1
Gravity intensity	Gravity intensity l	10
	Gravity intensity 2	9
	Gravity intensity 3	8
	Gravity intensity 4	7
	Gravity intensity 5	6
	Gravity intensity 6	5
	Gravity intensity 7	4
	Gravity intensity 8	3
	Gravity intensity 9	2
	Gravity intensity 10	1
Au anomaly	High anomaly	10
	Moderate anomaly	6
	Low anomaly	1
Ag anomaly	High anomaly	10
	Moderate anomaly	6
	Low anomaly	1
Cu anomaly	High anomaly	10
	Moderate anomaly	6
	Low anomaly	1
Mo anomaly	High anomaly	10
	Moderate anomaly	6
	Low anomaly	1
Pb anomaly	High anomaly	10
	Moderate anomaly	6
	Low anomaly	1
Zn anomaly	High anomaly	10
	Moderate anomaly	6
	Low anomaly	1

There are five fuzzy operators that are useful for integrating the weighted evidential layers to generate the final potential map: fuzzy AND, fuzzy OR, fuzzy algebraic product, fuzzy algebraic sum, and fuzzy gamma (γ) (An et al. 1991; Bonham-Carter 1994).

Prediction-area plot

The P-A method is a simple prediction rate-occupied area plot, which can be used not only to compare and evaluate the ability of different prospectivity models in predicting mineral deposits, but also to assign weights

Table 4 Consistency ratio (CR) for pairwise comparison matrix

CI	Criteria			Geological data			Geochemical data						Geophysical data		
	Geology	Geochemistry	Geophysics	Host rock	Heat source	Structure	Alteration	Au anomaly	Ag anomaly	Cu anomaly	Mo anomaly	Pb anomaly	Zn anomaly	Magnetic anomaly	Gravity anomaly
DM1	0.0370			0.0343				0.0236						0	
DM2	0.0036			0.0138				0.0169						0	
DM3	0.0053			0.0394				0.0092						0	

to evidential layers (Yousefi and Carranza 2014, 2015a, c; Parsa et al. 2016).

In a P-A plot, there are two curves, the curve of the percentage (prediction rate) of known mineral occurrences corresponding to the classes of the prospectivity map and the curve of the percentage of occupied areas corresponding to the classes of the prospectivity map. When an intersection point of the two curves is at a higher place in the P-A plot, it portrays a small area containing large number of mineral deposits. Furthermore, it chooses objectively a better model to give priority for mineral exploration (Yousefi and Carranza 2014, 2015a, c).

Application of the fuzzy AHP to porphyry-Cu deposits

Criteria for MPM

Considering expert opinions, the geological setting, the model of porphyry-Cu mineralization, a typical porphyry-Cu deposit, and the available data in the study area, three main criteria, including geological data, stream sediment geochemical data, and geophysical data, were used as input evidential layers to provide the mainstays in prospecting for porphyry-Cu deposits. The three main criteria consisted of (1) host rock lithology, (2) intrusive rock lithology as heat sources, (3) the density of faults and the distance to faults as structure, (4) different alteration zones, (5) geochemical anomalies of indicator elements Au, Ag, Cu, Mo, Pb, and Zn, and (6) the intensity of airborne magnetic and Bouguer gravity data, which are the most significant alternatives for exploration and characterization of porphyry-Cu deposits.

Preparation of evidential layers

Data preprocessing

The selection of evidential layers requires extensive consideration of the characteristics of porphyry-Cu deposits and the favorable conditions for mineralization. As discussed above, host rock lithology, intrusive rock lithology, alteration types, and faults were extracted and compiled from geological maps to obtain evidential layers.

The different types of intrusive rocks were extracted as separate maps, and each map of intrusive rocks and the host rock map were buffered into three zones, each 1 km wide, up to a distance of 3 km. Similarly, maps were generated for the different types of alteration, and these were buffered into three zones, each 0.5 km wide, up to a distance of 1.5 km. The density and distance of faults were analyzed by ArcGIS software. The density map was divided into nine equal-sized

Table 5 Fuzzy evaluation matrix with respect to criteria

	Geological data	Geochemical data	Geophysical data
Geological data	(1, 1, 1)	(2, 3.3333, 5)	(3, 4.3333, 5)
Geochemical data	(0.2, 0.3444, 0.5)	(1, 1, 1)	(0.3333, 0.8889, 2)
Geophysical data	(0.2, 0.2444, 0.3333)	(0.5, 1.3333, 3)	(1, 1, 1)

zones in the range 0–1.53 length per unit area, and values greater than 1.53 comprised the tenth zone. In this way, six 1-km-interval zones around the faults formed the sections of the distance map, and the seventh zone comprised area at a distance greater than 6 km.

Stream sediment geochemical anomalies were analyzed using the singularity mapping technique (Cheng 2007; Zuo et al. 2009). In simple terms, the element content of Au, Ag, Cu, Mo, Pb, and Zn were used as six other evidential layers, which were discretized into three classes. The thresholds of evidential layers corresponded to the second, fifth, and tenth quantiles. In addition, magnetic and gravity intensity data were assigned to ten classes, providing the evidential layers for airborne magnetic and Bouguer gravity data.

Data encoding

After categorizing evidential maps, the classes of the evidential maps must be ranked according to expert opinions of geoscientists. Based on Table 3, the above multi-class evidential maps were coded with integer values from 1 to 10. It should be noted that maps of different intrusive rocks, maps of different alterations, the density map, and the distance map were merged to generate the evidential layers for heat source, alteration, and structure. To simplify the process and improve efficiency, the above evidential layers were converted into grid format with a pixel size of 1 km.

Weights of evidential layers

In this study, three DMs with expertise in porphyry-Cu mineralization were invited to compare the relative importance of hierarchical elements using the scale in Table 1. In this phase, pairwise comparison matrices were formed to construct fuzzy evaluation matrices in case that CR ≤0.1.

All consistency ratios derived from the PCMs are less than 0.1 (Table 4). Consequently, the results were considered reasonable. The values of PCMs are then transformed into TFNs to construct fuzzy evaluation matrices presented in Tables 5, 6, 7, and 8.

After establishing fuzzy evaluation matrices, the weights of 12 evidential layers for mineral exploration can be calculated by the fuzzy AHP method. Taking geological alternatives as an example, details of calculating weights from the fuzzy evaluation matrix (Table 6) are given below.

From Eq. (6), the value of the fuzzy synthetic was computed as follows:

$$S_{\text{Host rock}} = (1.8095,\ 3.0698,\ 5.2)\otimes\left(\frac{1}{42.95},\frac{1}{29.1396},\frac{1}{17.6191}\right) = (0.0421,\ 0.1053,\ 0.2951)$$
$$S_{\text{Heat source}} = (12,\ 15.6667,\ 20)\otimes\left(\frac{1}{42.95},\frac{1}{29.1396},\frac{1}{17.6191}\right) = (0.2794,\ 0.5376,\ 1.1351)$$
$$S_{\text{Structure}} = (1.9167,\ 4.9833,\ 9.5)\otimes\left(\frac{1}{42.95},\frac{1}{29.1396},\frac{1}{17.6191}\right) = (0.0446,\ 0.1710,\ 0.5392)$$
$$S_{\text{Alteration}} = (1.8929,\ 5.4198,\ 8.25)\otimes\left(\frac{1}{42.95},\frac{1}{29.1396},\frac{1}{17.6191}\right) = (0.0441,\ 0.1860,\ 0.4682)$$

The degrees of possibility of these fuzzy values were then determined from Eq. (9) as follows:

$$V(S_{\text{Host rock}}\geq S_{\text{Heat source}}) = 0.035,\quad V(S_{\text{Heat source}}\geq S_{\text{Host rock}}) = 1$$
$$V(S_{\text{Host rock}}\geq S_{\text{Structure}}) = 0.7922,\quad V(S_{\text{Heat source}}\geq S_{\text{Structure}}) = 1$$
$$V(S_{\text{Host rock}}\geq S_{\text{Alteration}}) = 0.7567,\quad V(S_{\text{Heat source}}\geq S_{\text{Alteration}}) = 1$$
$$V(S_{\text{Structure}}\geq S_{\text{Host rock}}) = 1,\quad V(S_{\text{Alteration}}\geq S_{\text{Host rock}}) = 1$$
$$V(S_{\text{Structure}}\geq S_{\text{Heat source}}) = 0.4148,\quad V(S_{\text{Alteration}}\geq S_{\text{Heat source}}) = 0.3494$$
$$V(S_{\text{Structure}}\geq S_{\text{Alteration}}) = 0.9706,\quad V(S_{\text{Alteration}}\geq S_{\text{Structure}}) = 1$$

Finally, the weights were assigned and normalized using Eqs. (10) and (12):

$$V'(\text{Host rock}) = \min(0.035,\ 0.7922,\ 0.7567) = 0.035$$
$$V'(\text{Heat source}) = \min(1,\ 1,\ 1) = 1$$
$$V'(\text{Structure}) = \min(1,\ 0.4148,\ 0.9706) = 0.4148$$
$$V'(\text{Alteration}) = \min(1,\ 0.3494,\ 1) = 0.3494$$

The weights vector was (0.035, 1, 0.4148, 0.3494) and the normalized weights vector was calculated as (0.0195, 0.5558, 0.2305, 0.1492). In the same way, all normalized weights were obtained from fuzzy evaluation matrices. Final normalized weights for each criterion and alternative are presented in Table 9. It is apparent that heat source, structure, alteration,

Table 6 Fuzzy evaluation matrix with respect to geological alternatives

	Host rock	Heat source	Structure	Alteration
Host rock	(1, 1, 1)	(0.1429, 0.1810, 0.2)	(0.3333, 0.9444, 2)	(0.3333, 0.9444, 2)
Heat source	(5, 5.6667, 7)	(1, 1, 1)	(2, 4.3333, 6)	(4, 4.6667, 6)
Structure	(0.5, 1.8333, 3)	(0.1667, 0.2889, 0.5)	(1, 1, 1)	(0.25, 1.8611, 5)
Alteration	(0.5, 1.8333, 3)	(0.1429, 0.1865, 0.25)	(0.25, 2.4, 4)	(1, 1, 1)

Table 7 Fuzzy evaluation matrix with respect to geochemical alternatives

	Au anomaly	Ag anomaly	Cu anomaly	Mo anomaly	Pb anomaly	Zn anomaly
Au anomaly	(1, 1, 1)	(1, 2.3333, 3)	(0.1429, 0.2699, 0.3333)	(0.25, 0.75, 1)	(0.3333, 3.4444, 6)	(0.3333, 3.4444, 6)
Ag anomaly	(0.3333, 0.5556,1)	(1, 1, 1)	(0.1429, 0.1810, 0.2)	(0.25, 0.3056, 0.3333)	(0.3333, 1.7778, 3)	(0.3333, 1.7778, 3)
Cu anomaly	(3, 4.3333, 7)	(5, 5.6667, 7)	(1, 1, 1)	(2, 2.6667, 3)	(4, 6.6667, 9)	(6, 7.3333, 9)
Mo anomaly	(1, 2, 4)	(3, 3.3333, 4)	(0.3333, 0.3889, 0.5)	(1, 1, 1)	(2, 4, 6)	(2, 4, 6)
Pb anomaly	(0.1667, 1.1389, 3)	(0.1667, 1.1389, 3)	(0.1111, 0.1680, 0.25)	(0.1667, 0.3056, 0.5)	(1, 1, 1)	(1, 1.3333, 2)
Zn anomaly	(0.1667, 1.1389, 3)	(0.1667, 1.1389, 3)	(0.1111, 0.1402, 0.1667)	(0.1667, 0.3056, 0.5)	(0.5, 0.8333, 1)	(1, 1, 1)

and airborne magnetic data have higher values, so they play a significant role in prospecting for porphyry-Cu mineralization in the study area.

Integration of evidential layers

The corresponding evidential layers must be multiplied by final weights before employing fuzzy operators (Fig. 3). The evidential layers were combined using γ values of 0.78, 0.83, 0.88, and 0.93 to generate prospectivity maps (Fig. 4). Subsequently, these maps are divided into ten natural break (Jenks) classes. Each prospectivity map was evaluated and compared using the P-A plot. Figure 5 and Table 10 show that the prospectivity map obtained using a γ value of 0.83 was appropriate because it quantitatively depicts a smaller area containing the same number of mineral deposits. For further evaluation of this prospectivity map, the C-A model was used to determine the thresholds to defuzzify the map. The ternary map (Fig. 6) was generated using two thresholds, shown in Fig. 7, which identified the appropriate areas for porphyry-Cu mineralization.

Results and discussion

As mentioned above, the AHP's pairwise comparison is made in crisp values, relying on expert knowledge. Any incorrect opinions of the expert can convey into the assignment of weights. In this process, the vagueness and uncertainty introduced into pairwise matrix lead to the difficulty providing exact weights for evidential layers (Feizizadeh and Blaschke 2013; Feizizadeh et al. 2014). To overcome this problem, fuzzy AHP use TFNs to simulate DMs' preference in pairwise comparison process. In the fuzzy AHP method, each choice of the relative importance of hierarchy criteria is expressed by a vector, which is better to simulate human judgment than crisp comparison. Therefore, the fuzzy AHP method can provide more realistic weights than other knowledge-driven MPM methods

One of the key procedures in the implementation of the fuzzy AHP modeling is the selection of fuzzy operators. Knox-Robinson (2000) pointed out that fuzzy γ operator is useful and realistic, which focuses on balancing the "decreasive" and "increasive" effects of fuzzy algebraic product and fuzzy algebraic sum operators. Using appropriate values of γ can control the propagation of extreme-value noise to the final prospectivity map (Porwal et al. 2003b). The ultimate aim for carefully tempering the value of γ is to select one that provides the "best" result. A number of γ were tried, values of 0.78, 0.83, 0.88, and 0.93 were selected to generate prospectivity maps. However, Fig. 4 shows that the prospectivity maps for different γ values are remarkably similar. For avoiding subjective judgment, the P-A method (Yousefi and Carranza 2014, 2015a, b, c; Yousefi and Nykänen 2015) is used to select the "best" result. Consequently, the result of applying a γ value of 0.83 is the best one in that it reduces the target area of the study area

Table 8 Fuzzy evaluation matrix with respect to geophysical alternatives

	Magnetic anomaly	Gravity anomaly
Magnetic anomaly	(1, 1, 1)	(1, 2, 3)
Gravity anomaly	(0.3333, 0.6111, 1)	(1, 1, 1)

Table 9 Weights of criteria and alternatives

Criterion	Weight	Alternative	Weight	Final weight
Geological data	0.7292	Host rock	0.0195	0.0142
		Heat source	0.5558	0.4052
		Structure	0.2305	0.1681
		Alteration	0.1942	0.1416
Geochemical data	0.0841	Au anomaly	0.3482	0.0293
		Ag anomaly	0.0050	0.0004
		Cu anomaly	0.3695	0.0311
		Mo anomaly	0.2340	0.0197
		Pb anomaly	0.0351	0.0030
		Zn anomaly	0.0082	0.0007
Geophysical data	0.1867	Magnetic anomaly	0.6805	0.1270
		Gravity anomaly	0.3195	0.0597

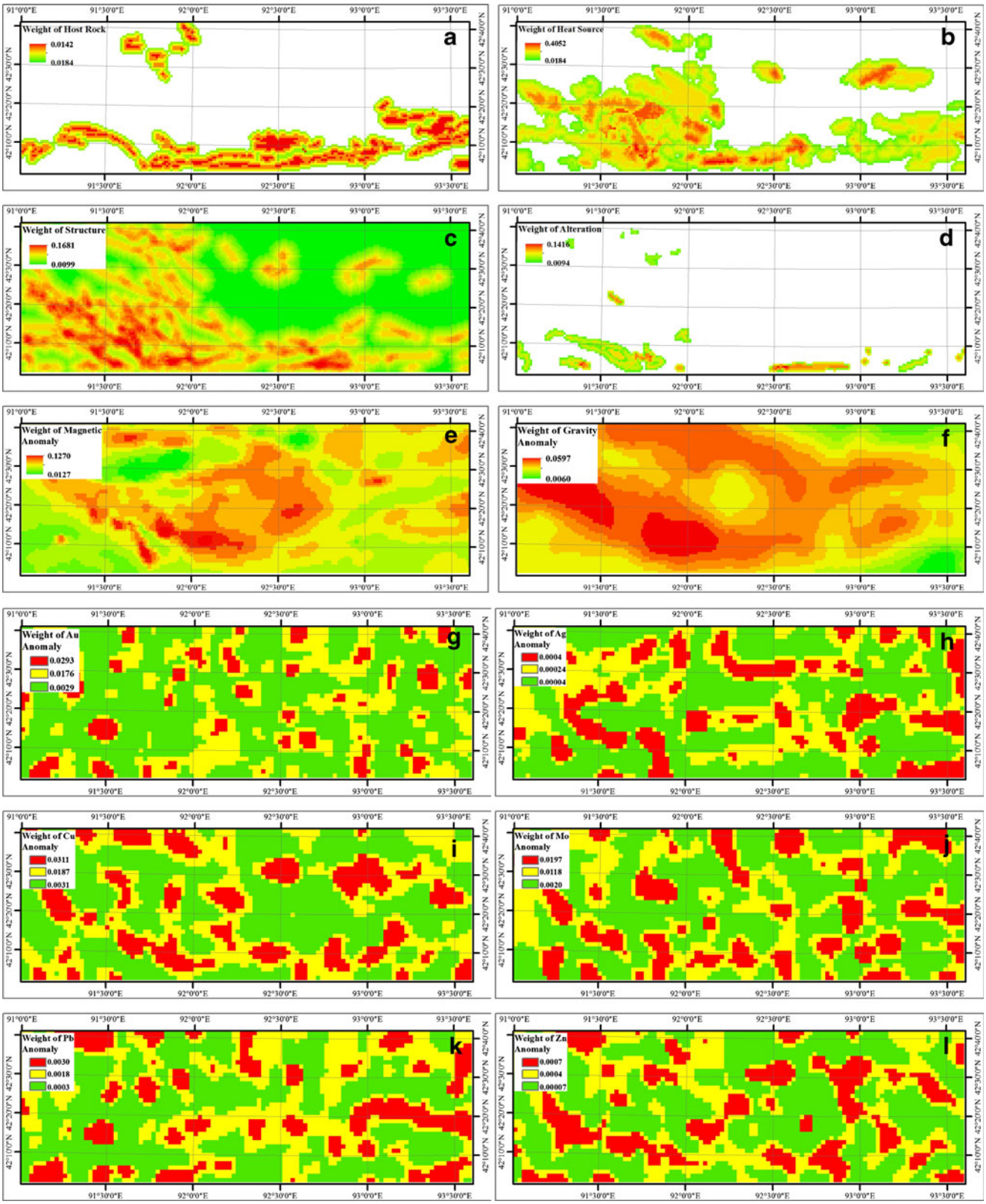

Fig. 3 Weighted evidential layers: **a** Host rock, **b** Heat source, **c** Structure, **d** Alteration, **e** Magnetic anomaly, **f** Gravity anomaly, **g** Au anomaly, **h** Ag anomaly, **i** Cu anomaly, **j** Mo anomaly, **k** Pb anomaly, and **l** Zn anomaly

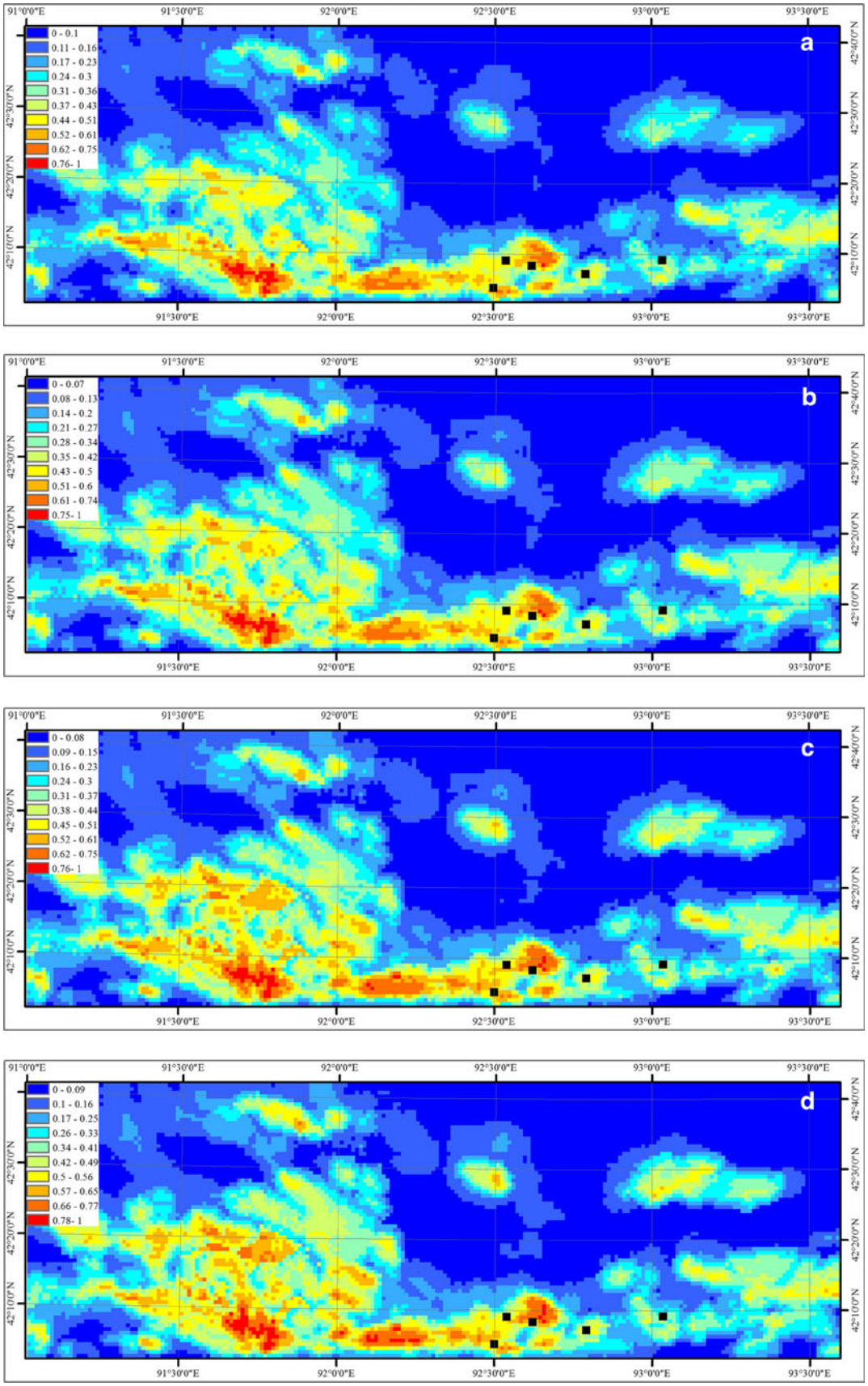

Fig. 4 Prospectivity maps obtained using γ values of **a** 0.78, **b** 0.83, **c** 0.88, and **d** 0.93

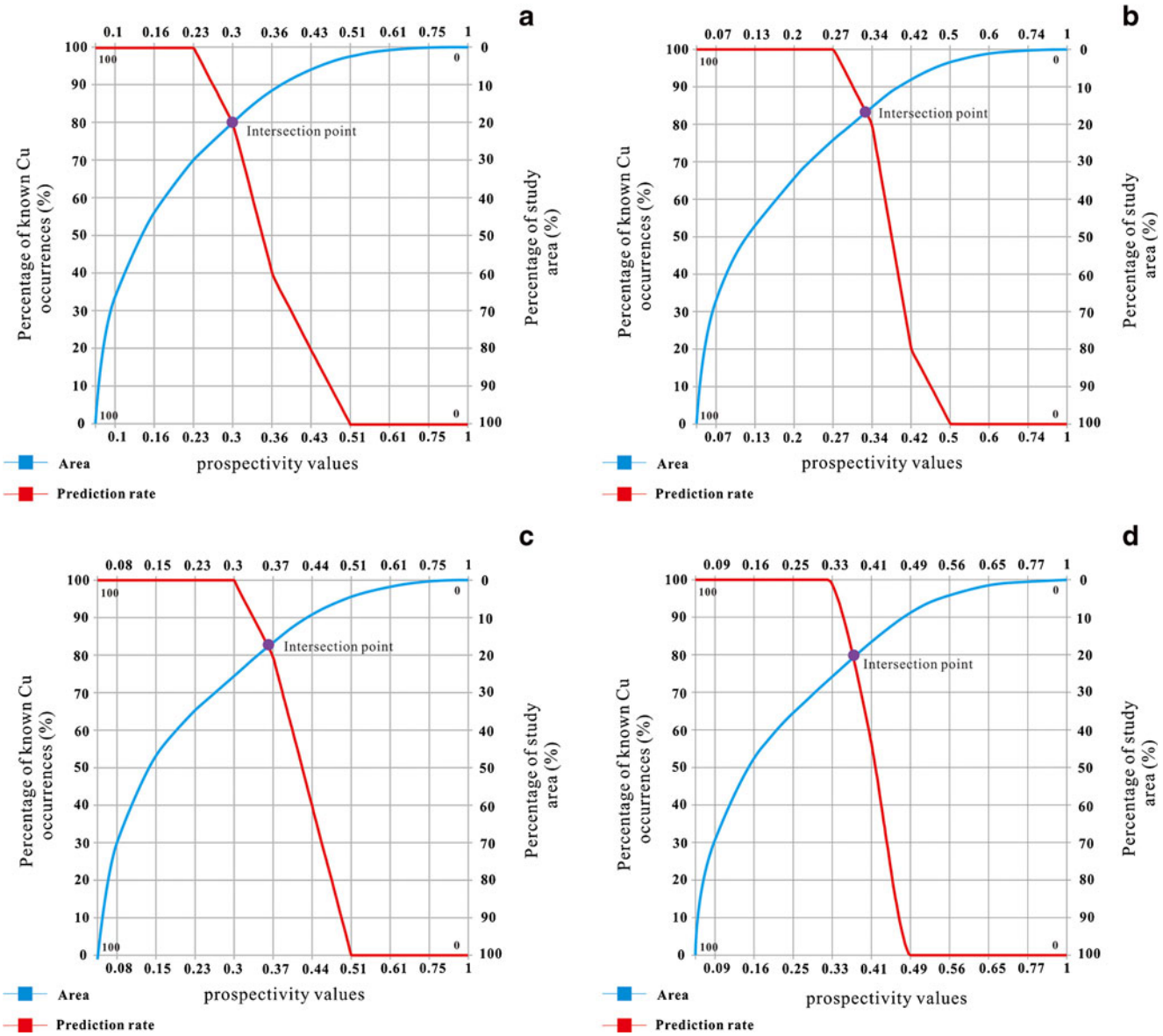

Fig. 5 Prospectivity maps obtained using γ values of **a** 0.78, **b** 0.83, **c** 0.88, and **d** 0.93

while predicting the same number of known deposits, and it is meaningful in mineral exploration.

In the ternary map, high favorability zones occupy only 7.16 % of the study area, and these zones are mostly in the south and southwest; the moderate favorability zones are mainly close to the high favorability zones, occupying 18.61 % of the study area. The spatial distribution of high favorability zones is confined to specific intrusive rocks with a composition of diorite and monzodiorite, which emphasizes a strong heat sources control of porphyry-Cu mineralization in the study area. This conforms to characterizations of spatial associations between geological features and porphyry-Cu deposits. However, it fails to predict the Chihu deposit, a small, low-grade porphyry-Cu deposit, in high favorability zone. The metallogenetic epoch and the metallotectonic setting of the Chihu deposit, discovered in 1986, are uncertain as its formation age is vigorously debated (Ji and Sun 2011; Wu et al. 2006). Therefore, it is difficult to predict such a deposit in high favorability zones based on regional scale data and criteria for MPM. The larger scale data and local scale criteria

Table 10 Extracted parameters from intersection point of P-A plots in Figure 5

Prospectivity map	Prediction rate (%)	Threshold	Occupied area (%)
Gamma γ = 0.78	79.9	0.3	20.1
Gamma γ = 0.83	84	0.33	16
Gamma γ = 0.88	82.2	0.36	17.8
Gamma γ = 0.93	78.5	0.38	21.5

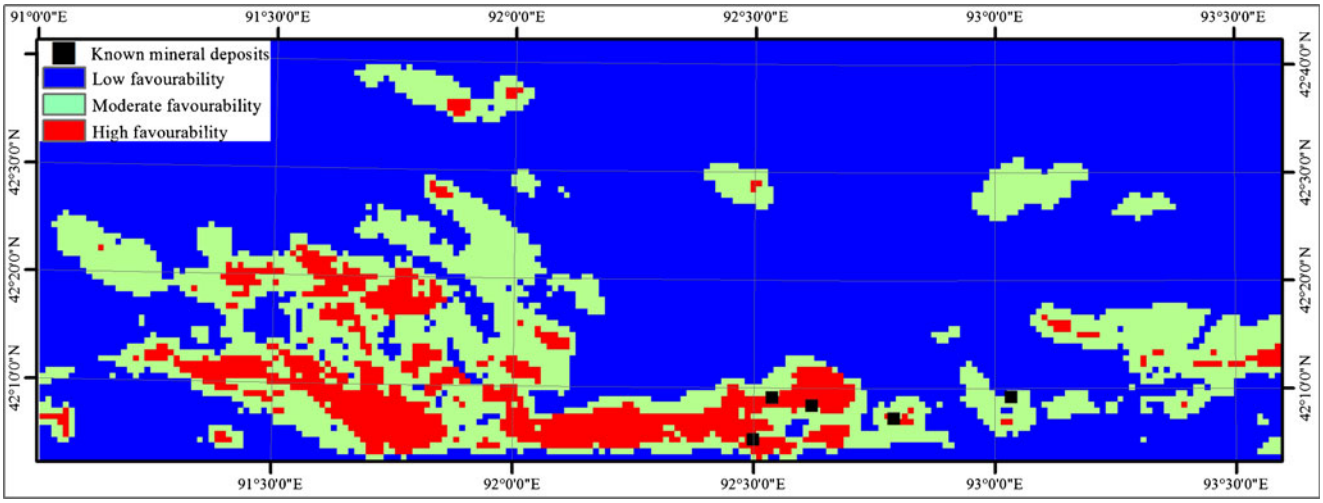

Fig. 6 Ternary prospectivity map generated by defuzzification of the prospectivity map (Fig. 4b)

for porphyry-Cu mineralization are synthesized to predict the Chihu deposit and demarcate other prospects within the predicted potential targets for guiding follow-up exploration using the same method. Therefore, high favorability zones and the specific moderate favorability area containing the Chihu deposit should be prioritized in the exploration of porphyry-Cu deposits.

The study area with only five porphyry-Cu deposits restricted the validation of prospectivity model using the known mineral deposits. From the perception of spatial domain, the spatial distribution of high favorability zones is in conformity with the model of porphyry-Cu mineralization. It well illustrates the effectiveness of fuzzy AHP method for porphyry-Cu deposits in this study. In addition, field observations will be used to evaluate target areas in the future.

Conclusions

1. The application of the fuzzy AHP approach simulates human judgment for the relative importance of hierarchy criteria, as well as reducing the vagueness and uncertainty of crisp comparison via the triangular fuzzy numbers. Furthermore, more realistic weights for evidence layers are provided than those given by other knowledge-driven MPM methods.
2. A key element of the proposed approach is the use of different values of γ to obtain the most suitable potential map, which has an advantage over other knowledge-driven MPM methods in that it avoids subjective opinions when selecting the final potential map.
3. The P-A plot provides an objective method to weight the relative effectiveness in terms of reducing the exploration area while decreasing the exploration costs, when the prospectivity maps for different values of γ are remarkably similar.
4. The ternary map shows a strong spatial correlation between high favorability zones and specific intrusive rocks composed of diorite and monzodiorite, which is consistent with the model of porphyry-Cu mineralization, thus, the fuzzy AHP method for mapping prospectivity for porphyry-Cu deposits is valid in this study.
5. In this study, potential targets are delineated in the Dananhu metallogenic belt. For obtaining a more detailed

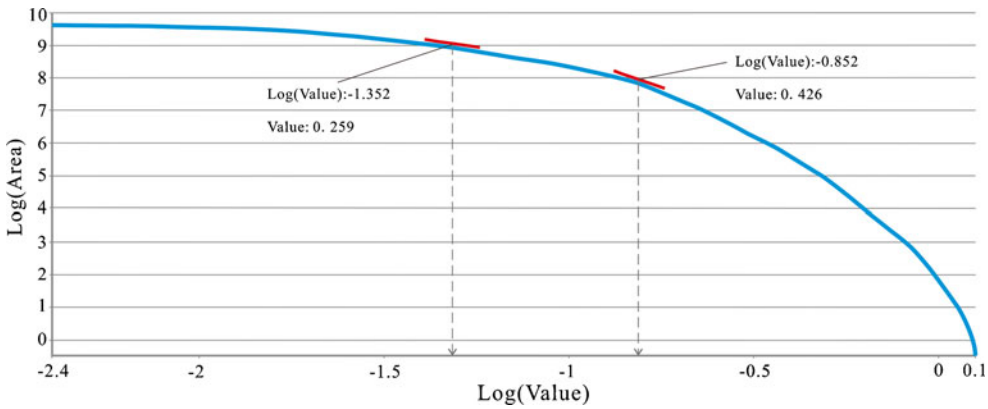

Fig. 7 Concentration-area (C-A) model for the prospectivity map (Fig. 4b)

result, with the larger scale data, the same method needs to further delineate other prospects within the predicted potential targets to guide follow-up exploration.

6. The fuzzy AHP method described in this paper provides a simple yet effective method for prioritizing potential targets in "greenfield" areas.

Acknowledgments The authors thank anonymous reviewers for their constructive comments and suggestions. This research benefited from the support from major projects in the Xinjiang Uygur Autonomous Region (201330121-3), Cooperative program of Chinese Academy of Sciences and Local Government (the science and technology program aims to support the development of Xinjiang), National Basic Research Program of China 973 Program (2014CB440803), Funded projects for the western Dr. (XBBS201203), and 100 Talents Program of Xinjiang.

References

Abedi M, Norouzi GH, Fathianpour N (2013a) Fuzzy outranking approach: a knowledge-driven method for mineral prospectivity mapping. Int J Appl Earth Obs Geoinf 21:556–567

Abedi M, Torabi SA, Norouzi GH (2013b) Application of fuzzy AHP method to integrate geophysical data in a prospect scale, a case study: seridune copper deposit. Boll Geofis Teor Appl 54:145–164

Agterberg FP, Bonham-Carter GF (1999) Logistic regression and weights of evidence modeling in mineral exploration. In: Proceedings APCOM '99, Colorado School of Mines. Golden, Colorado

Albayrak E, Erensal Y (2004) Using analytic hierarchy process (AHP) to improve human performance: an application of multiple criteria decision making problem. J Intell Manuf 15:491–503

An P, Moon WM, Rencz A (1991) Application of fuzzy set theory for integration of geological, geophysical and remote sensing data. Can J Explor Geophys 27:1–11

Bonham-Carter GF (1994) Geographic information systems for geoscientists: modeling with GIS. Pergamon Press, Oxford

Buckley JJ (1985) Fuzzy hierarchical analysis. Fuzzy Sets Syst 17:233–247

Carranza EJM (2008) Geochemical anomaly and mineral prospectivity mapping in GIS. In: Handbook of exploration and environmental geochemistry. Elsevier, Amsterdam, p 368

Carranza EJM (2010) Improved wildcat modelling of mineral prospectivity. Resour Geol 60:129–149

Carranza EJM (2014) Evidential belief predictive modeling of mineral prospectivity using few prospects and evidence with missing values. Nat Resour Res. doi:10.1007/s11953-014-9250-z

Carranza EJM, Hale M (2001) Logistic regression for geologically constrained mapping of gold potential, Baguio district, Philippines. Explor Min Geol 10:165–175

Carranza EJM, Hale M (2002) Wildcat mapping of gold potential, Baguio district, Philippines. Appl Earth Sci 111:100–105

Carranza EJM, Hale M (2003) Evidential belief functions for data-driven geologically constrained mapping of gold potential, Baguio district, Philippines. Ore Geol Rev 22:117–132

Carranza EJM, Mangaoang JC, Hale M (1999) Application of mineral exploration models and GIS to generate mineral potential maps as input for optimum land-use planning in the Philippines. Nat Resour Res 8:165–173

Chang D (1996) Applications of the extent analysis method on fuzzy AHP. Eur J Oper Res 95:649–655

Chen Y (2006) Mineral resource and metallogenetic system in Tianshan, China. Geological Press, Beijing **(in Chinese)**

Cheng Q (2007) Mapping singularities with stream sediment geochemical data for prediction of undiscovered mineral deposits in Gejiu, Yunnan Province, China. Ore Geol Rev 32:314–324

Cheng Q, Agterberg F, Ballantyne S (1994) The separation of geochemical anomalies from background by fractal methods. J Geochem Explor 51:109–130

Dagdeviren M (2008) Decision making in equipment selection: an integrated approach with AHP and PROMETHEE. J Intell Manuf 19: 397–406

Dong L, Feng J, Liu D, Tang Y, Qu X, Wang K, Yang Z (2010) Research for classification of metallogenic unit of Xinjiang. Xinjiang Geol 28: 1–15 **(in Chinese)**

Feizizadeh B, Blaschke T (2013) Land suitability analysis for Tabriz County, Iran: a multi-criteria evaluation approach using GIS. J Environ Plan Manag 56:1–23

Feizizadeh B, Roodposhti MS, Jankowski P, Blaschke T (2014) A GIS-based extended fuzzy multi-criteria evaluation for landslide susceptibility mapping. Comput Geosci 73:208–221

Han C, Xiao W, Zhao G, Mao J, Wang Z, Yan Z, Mao Q (2006) Geological characteristics and genesis of the Tuwu porphyry copper deposit, Hami, Xinjiang, Central Asia. Ore Geol Rev 29:77–94

Ji H, Sun J (2011) Discussion on characteristics and metallogenic epoch of Chihu Cu–Mo deposits in Hami, Xinjiang. Acta Miner Sin S: 595–596 (in Chinese)

Karimi AR, Mehrdadi N, Hashemian SJ, Nabi-Bidhendi GR, Tavakkoli-Moghaddam R (2011) Using of the fuzzy TOPSIS and fuzzy AHP methods for wastewater treatment process selection. Int J academic res 3:737–745

Knox-Robinson CM (2000) Vectorial fuzzy logic: a novel technique for enhanced mineral prospectivity mapping, with reference to the orogenic gold mineralisation potential of the Kalgoorlie Terrane, Western Australia. Aust J Earth Sci 47:929–941

Lindsay MD, Betts PG, Ailleres L (2014) Data fusion and porphyry copper prospectivity models, southeastern Arizona. Ore Geol Rev 61:120–140

Liu D, Chen Y, Wang D, Tang Y, Zhou R, Wang J, Li H, Chen F (2003) A Discussion on problems related to mineralization of Tuwu-Yandong Cu-Mo orefield in Hami, Xinjiang. Miner Depos 22:334–344 **(in Chinese)**

Liu Y, Cheng Q, Xia Q, Wang X (2014) Mineral potential mapping for tungsten polymetallic deposits in the Nanling metallogenic belt, South China. J Earth Sci 25:689–700

Liu Y, Cheng Q, Xia Q, Wang X (2015) The use of evidential belief functions for mineral potential mapping in the Nanling belt, South China. Front Earth Sci 9:342–354

Mao J, Goldfarb RJ, Wang Y, Hart CJ, Wang Z, Yang J (2005) Late Paleozoic base and precious metal deposits, East Tianshan, Xinjiang, China: Characteristics and geodynamic setting. Episodes 28:23–30

Najafi A, Karimpour MH, Ghaderi M (2014) Application of fuzzy AHP method to IOCG prospectivity mapping: a case study in Taherabad prospecting area, eastern Iran. Int J Appl Earth Obs Geoinf 33:142–154

Parsa M, Maghsoudi A, Yousefi M, Sadeghi M (2016) Prospectivity modeling of porphyry-Cu deposits by identification and integration of efficient mono-elemental geochemical signatures. J Afr Earth Sci 114:228–241

Pazand K, Hezarkhani A, Ghanbari Y (2014) Fuzzy analytical hierarchy process and GIS for predictive Cu porphyry potential mapping: a case study in Ahar-Arasbaran Zone (NW, Iran). Arab J Geosci 7: 241–251

Porwal A, Carranza EJM, Hale M (2003a) Artificial neural networks for mineral potential mapping: a case study from Aravalli Province, Western India. Nat Resour Res 12:155–171

Porwal A, Carranza EJM, Hale M (2003b) Knowledge-driven and data-driven fuzzy models for predictive mineral potential mapping. Nat Resour Res 12:1–25

Rui Z, Wang L, Wang Y, Liu Y (2002a) Discussion on metallogenic epoch of Tuwu and Yandong porphyry copper deposits in East Tianshan Mountains, Xinjiang. Miner Depos 21:16–22 **(in Chinese)**

Rui Z, Liu Y, Wang L, Wang Y (2002b) The eastern Tianshan porphyry copper belt in Xinjiang and its tectonic framework. Acta Geol Sin 76:83–94 **(in Chinese)**

Saaty TL (1980) The analytic hierarchy process, planning, piority setting, resource allocation. McGraw-Hill, New York

Singer DA, Kouda R (1996) Application of a feedforward neural network in the search for Kuroko deposits in the Hokuroku district, Japan. Math Geol 28:1017–1023

Van Laarhoven PJM, Pedrycz W (1983) A fuzzy extension of Saaty's priority theory. Fuzzy Sets Syst 11:199–227

Wang F, Feng J, Hu J, Wang L, Jiang L, Zhang Z (2001) The characteristics and significance of Tuwu large-type porphyry copper deposit in Xinjiang. Chin Geol 28:36–39+29 **(in Chinese)**

Wang Y, Luo Y, Hua Z (2008) On the extent analysis method for fuzzy AHP and its applications. Eur J Oper Res 186:735–747

Wang Y, Xue C, Liu J, Wang J, Yang J, Zhang F, Zhao Z, Zhao Y, Zhao Y, Liu B (2015) Early Carboniferous adakitic rocks in the area of the Tuwu deposit, eastern Tianshan, NW China: slab melting and implications for porphyry copper mineralization. J Asian Earth Sci 103:332–349

Wu H, Li H, Chen F, Lu Y, Deng G, Mei Y, Ji H (2006) Zircon SHRIMP U-Pb dating of plagiogranite porphyry in the Chihu molybdenum-copper district, Hami, East Tianshan. Geol bull Chin 25:549–552 **(in Chinese)**

Xiao F (2013) Mineral resource asseaament in covered area: a case study from "Tuwu-type" porphyry Cu-Mo deposits in Gobi desert landscape of eastern Tianshan, China. Ph.D. thesis, China University of Geosciences, Wuhan, China **(in Chinese)**

Xie X, Mu X, Ren X (1997) Geochemical mapping in China. J Geochem Explor 60:99–113

Xu R (2000) Fuzzy least-squares priority method in the analytic hierarchy process. Fuzzy Sets Syst 112:395–404

Yousefi M, Carranza EJM (2014) Data-driven index overlay and Boolean logic mineral prospectivity modeling in greenfields exploration. Nat Resour Res. doi: 10.1007/s11053-014-9261-9.

Yousefi M, Carranza EJM (2015a) Fuzzification of continuous-value spatial evidence for mineral prospectivity mapping. Comput Geosci 74:97–109

Yousefi M, Carranza EJM (2015b) Geometric average of spatial evidence data layers: a GIS-based multi-criteria decision-making approach to mineral prospectivity mapping. Comput Geosci 83:72–79

Yousefi M, Carranza EJM (2015c) Prediction-area (P-A) plot and C-A fractal analysis to classify and evaluate evidential maps for mineral prospectivity modeling. Comput Geosci 79:69–81

Yousefi M, Nykänen V (2015) Data-driven logistic-based weighting of geochemical and geological evidence layers in mineral prospectivity mapping. J Geochem Explor doi:10.1016/j.gexplo.2015.10.008

Zhang L, Xiao W, Qin K, Zhang Q (2006) The adakite connection of the Tuwu-Yandong copper porphyry belt, eastern Tianshan, NW China: trace element and Sr-Nd-Pb isotope geochemistry. Miner Depos 41: 188–200

Zhu Y, Wang F, Long B, Xue Y, Xiao K, Feng J, Zhuang D, Jiang L (2003) Polygenic information prospecting model for Tuwu-Yandong porphyry Cu-Mo deposits. Miner Depos 22:287–294 **(in Chinese)**

Zhuang D (2003) The geochemical characteristics and anomoly verification methods of Tuwu and Yandong copper-deposits in the eastern Tianshan mountains, Xingjiang. Geol Prospect 39:67–71 **(in Chinese)**

Zhuang D, Wang S, Jiao X (2003) The predicting model of the synthetic information on Tuwu and Yandong copper orefield. Xinjiang Geol 21:293–297 **(in Chinese)**

Zuo R (2011) Regional exploration targeting model for Gangdese porphyry copper deposits. Resour Geol 61:296–303

Zuo R, Cheng Q, Agterberg FP, Xia Q (2009) Application of singularity mapping technique to identify local anomalies using stream sediment geochemical data, a case study from Gangdese, Tibet, western China. J Geochem Explor 101:225–235